

# pH-Reversed ionic current rectification displayed by conically shaped nanochannel without any modification†

Zhijun Guo, Jiahai Wang,\* Jiangtao Ren and Erkang Wang\*

Received 28th April 2011, Accepted 17th June 2011

DOI: 10.1039/c1nr10434a

Ion current through a nascent nanochannel with conically shaped geometry in PET (polyethylene terephthalate) membrane sandwiched between two same buffer solutions at  $\text{pH} \leq 3$  was routinely considered to exhibit no rectification and, if any, much weaker rectification than that for a nanochannel with a negative surface charge, since the surface charge on the membrane decreases to zero along with decreasing the pH value of the buffer solution down to the  $\text{p}K_{\text{a}}$  of carboxylic acid. However, in this study, we discovered that in the buffer solution with low ionic strength at pH values below 3, the conically shaped nanochannels exhibited distinct ion current rectification, as expected for nanochannels with a positive surface charge, if voltages beyond  $\pm 2\text{V}$  range were scanned. We reasoned that the current rectification engendered by the positive surface charge of a conical nanochannel was due to further protonation of the hydrogen bonded hydrogel layer or neutral carboxylic acid inside the nanochannel. Therefore, our results enrich the knowledge about nanochannel technology and indicate that a nanofluidic diode based on pH-reversed ion current rectification through a conical nanochannel can be achieved without any modification of the PET membrane.

## 1. Introduction

A track-etching technique has been widespread in recent years used for fabrication of “abiotic” asymmetric conically shaped nanochannels,<sup>1–11</sup> which have been proved to be a versatile platform for biosensor and single molecule analysis. The asymmetric nanochannels possess analogous functions to a biological protein ion channel,<sup>12–19</sup> such as ion selectivity, current rectification, current fluctuation and current switch. On the basis of these outstanding physicochemical properties of asymmetric nanochannels embedded in the membrane, a series of investigations have been dedicated into looking for new tools for engineering these nanochannels with new functionalities similar to those of biological protein nanopores, and constructing nanofluidic devices by manipulating the ionic transport characteristics of conical nanochannels.<sup>8,20–25</sup>

Nanofluidic devices with tuned ionic selectivity and current rectification are extremely interesting, because they are responsive to user input and environmental surroundings, which is needed in real applications. The first example reported by Wei, Bard, and Feldberg in 1997 has demonstrated that a conically

shaped glass nanopipette rectified current with non-ohmic ion transport,<sup>26</sup> which sparked intensive research in this area.<sup>27–41</sup> Later, several other groups have demonstrated that a conically shaped nanochannel embedded in a polymer membrane had the same ion transport characteristics when transmembrane potential difference was applied.<sup>5,6,42,43</sup> The conically shaped nanochannel can also be made intelligent by functionalization of the nanochannel with a series of chemical groups, such as DNA,<sup>44,45</sup> polymer brush<sup>9,21</sup> and protein.<sup>24</sup> For example, Jiang's group have reported a series of smart nanochannel devices which are responsive to different stimuli,<sup>46–48</sup> such as pH,<sup>49</sup> potassium ion<sup>50</sup> and temperature.<sup>4</sup>

Among those investigations focusing on nanochannels in polymer membranes,<sup>3,4,9,20–24,42,51,52</sup> the PET membrane has been used to investigate the physical basis of ion transport across a biomimetic nanochannel embedded in the membrane, due to its dramatic advantages as compared to others. Firstly, the ease of etching a heavy ion track in the PET membrane only entails placing sodium hydroxide on one side<sup>53</sup> or on both sides of the membrane.<sup>1</sup> Secondly, the etching process can be closely monitored *via* recording currents; therefore, the small opening of the nanochannel can be adjusted at will by stopping the etching process at a desired current value corresponding to the expected diameter of the small opening of a conically shaped nanochannel. Finally, the surface of PET after etching using high concentration of sodium hydroxide is ended with a carboxyl group, which facilitates further functionalization of the inner channel wall. In combination with other various tools, various methods have

State Key Laboratory of Electroanalytical Chemistry, Changchun Institute of Applied Chemistry, Chinese Academy of Sciences, Graduate School of the Chinese Academy of Sciences, Changchun, 130022, Jilin, PR China. E-mail: jhwang@ciac.jl.cn; ekwang@ciac.jl.cn

† Electronic supplementary information (ESI) available: SEM images of multi-tracked nanochannel fabricated from a surfactant-protected one-step etching method. See DOI: 10.1039/c1nr10434a

been reported to chemically modify the surface wall of the nanochannel to tune the ion transport. The Martin group has invented a gold plating method to deposit a gold nanotube inside the nanochannels in the membrane, followed by modification with cysteine whose charge polarity can be switched by pH.<sup>54</sup> By finely adjusting the pH values, the transporting properties can be modulated. Alternative methods by using EDC/NHS coupling agent have also been utilized to efficiently functionalize the nanochannel with interesting functional groups.<sup>1,4,20,43</sup> In addition to the chemical modification of the nanochannel wall with charged groups, polyvalent ions have been demonstrated to reversibly bind a carboxyl group on the nanochannel wall, resulting in the reversal of the surface charge such that the current flow and current rectification can be adjusted without any chemical modification.<sup>3</sup> Adsorption of a hydrophobic drug with positive charge polarity onto the tip side of the nanochannel has also been reported to induce the local charge inversion in the nanopore wall, leading to switching of the ionic selectivity of the nanochannel from a positive ion to a negative ion.<sup>7</sup>

In this study, we demonstrated that even without chemical functionalization and existence of polyvalent ions (or hydrophobic molecules), a synthetic conical nanochannel in the PET membrane exhibited current rectifications in the solution at  $\text{pH} \leq 3$  as expected for the conical nanochannels with a positively charged surface. As is well known, ion current through a conically shaped nanochannel in the PET membrane sandwiched between two same solutions at  $\text{pH} \leq 3$  was routinely considered to exhibit no rectification and if any, much weaker rectification than that for a negatively charged surface, since the surface charge on the membrane is neutralized along with decreasing the pH value of the buffer solution down to the  $\text{p}K_{\text{a}}$  of carboxylic acid. However, in this study, we discovered that in solutions at  $\text{pH} \leq 3$ , the conically shaped nanochannels exhibited distinct positive ionic-current rectification, if voltages beyond  $\pm 2\text{V}$  range were scanned. We reasoned that the positive current rectification engendered by the positive charge of the surface of the conical nanochannel was due to further protonation of the hydrogen bonded hydrogel layer or neutral carboxylic acid inside the nanochannel.<sup>55–58</sup> Therefore, pH-reversed ionic-current rectification of a conical nanochannel can be achieved without any modification of the PET membrane.

## 2. Experimental

### Materials

PET (polyethylene terephthalate) membranes (diameter = 3 cm, thickness = 12  $\mu\text{m}$ ) that had been irradiated with a heavy ion of 2.2 GeV kinetic energy to create a single damage track through the membrane were obtained from GSI, Darmstadt, Germany and referred to as “tracked” membranes. Tetrakis (diisopropylguanidino)zinc phthalocyanine (Zn-DIGP) was provided by Prof. Nathan W. Luedtke, University of Zurich.<sup>59</sup> The surfactant DOWfax 2A1 was purchased from DOW Chemical. Sodium chloride (NaCl) and potassium chloride (KCl) were purchased from Beijing Chemical Reagent Company (Beijing, China). All of the chemicals were at least analytical grade. The water used throughout all experiments was purified by a Milli-Q system (Millipore, Bedford, MA, USA).

### Nanochannel fabrication

Nanochannels with a tip diameter of 1.5 nm and 3 nm were fabricated with two-step etching described by the Martin group for reproducibly preparing conically shaped nanochannels in tracked poly(ethylene terephthalate) membranes.<sup>60</sup> Each side of the tracked PET membrane was irradiated under UV light (365 nm) for 1 h, and then the membrane was mounted in a two-compartment cell such that the electrolyte solution could be placed on either side of the tracked membrane. The first etch step entailed placing an etching solution (9M NaOH) on one side of the membrane and a stopping solution that neutralizes the etchant (1M HCOOH and 1M KCl) on the other side. The temperature during etching was maintained at 20 °C. Each half cell contained a Pt wire (dia = 0.1 cm, length  $\sim 5$  cm), and a Keithley 2635A picoammeter/voltage-source (Keithley Instruments, Cleveland, OH) was used to apply a transmembrane potential of 1 V during etching and measure the resulting current ionic flowing through the nascent nanochannel. This first etch step was terminated when the current increased up to 0.1 nA. The stop solution was placed in both half cells to neutralize the etchant solution. According to a previous procedure, the diameter of the base opening after the first etch step was determined by obtaining scanning electron micrographs of the base side of multi-tracked PET membranes ( $1 \times 10^8$  tracks  $\text{cm}^{-2}$ ) etched under the same conditions. These studies yielded an etch rate of 2.3  $\text{nm min}^{-1}$ . The tip diameter was finely tuned by using a second etch step. The second etch step entailed placing the 1M NaOH etch solution on both sides of the membrane. A transmembrane potential of 1 V was applied. The etch step was stopped once the desired current corresponding to a certain tip diameter was reached.

Nanochannels with a tip diameter of 30 nm were fabricated using the surfactant-protected one-step etching method described by Ali for preparing conically shaped nanochannels in tracked poly(ethylene terephthalate) membranes.<sup>1</sup> The protecting solution (6 M NaOH + 0.07% 2A1) was placed on one side of the membrane, 6 M sodium hydroxide solution was placed on the UV-treated side to control the diameter of the big opening of the nanochannel. During the etching process, temperature was maintained at 40 °C. When the desired current was reached, 1 M HCl solution was placed on both sides of the membrane to stop the etching process. The other procedures were the same as those for the two-step etching method.

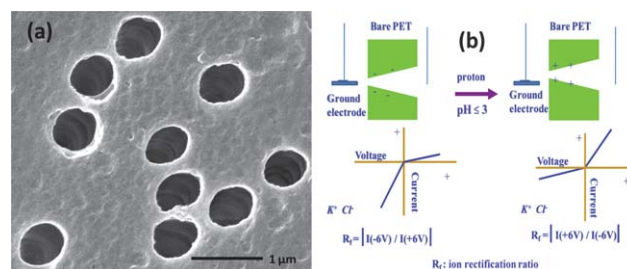


**Fig. 1** (a) Scanning electron microscopy of the base side of the conical nanochannel in a PET membrane *via* the two-step etching method. (b) Schematic illustration of switching the current–voltage curve in response to the reversal of charge polarity in the nanochannel.

Fig. 1(a) shows a SEM image of the base side of a multi-tracked membrane, and the average diameter ( $D$ ) of the base side is 550 nm. The tip diameter ( $d$ ) after the second etching was measured using the electrochemical method described in detail previously. The following equation was used to calculate the tip diameter:

$$d = 4LI/\pi DkV$$

where  $L$  is the membrane thickness,  $k$  is the conductivity of the electrolyte,  $V$  is the transmembrane voltage, and  $I$  is the ionic current. The equation provides a solution to obtaining the tip diameter of an ideal conically shaped nanochannel. However, the tip diameter cannot be directly imaged by the current techniques; therefore, a rough estimation of the tip diameter has to be used. The diameter of the nanochannel with surfactant protected etching was obtained in the same way as with the two-step etching method.

### Current–voltage measurement

To verify the successful fabrication of conically shaped nanochannels, an electrochemical measurement was carried out to characterize the current rectification which is an intriguing feature of the nascent nanochannel. Two silver/silver chloride electrodes were immersed on the tip side and the base side of the nanochannel, respectively. The current–voltage curves of an asymmetrical conical nanochannel were obtained by applying transmembrane potential differences in various buffer solutions. The current–voltage curves of the as-prepared nanochannel after adsorption of Zn-DIGP were measured in 20 mM phosphate buffered solution containing 10 mM KCl, as shown in Fig. 2.

### 3. Results and discussion

Nanoscale control of the surface charge in the nanochannel has been assessed as an effective method to modulate the ion transport through nanochannels and current rectification of nanochannels.<sup>3</sup> From all the studies involving nanochannels with surface modification and without modification, they showed that current rectification was very sensitive to the nanochannel charge and slight variation of the surface charge can trigger a distinct

change of the current rectification.<sup>61</sup> Therefore, the current rectification of the nanochannel is a paramount indicator of successful engineering of the inside of a conically shaped nanochannel and the sign of a surface charge. As shown in Fig. 1(b), the ground electrode is placed on the tip side of the nanochannel and the ion current rectification is dictated by the sign of the surface charge: a synthetic conical nanochannel with a negatively charged surface rectify the current such that the ion current flowing at a negative applied potential overwhelms the ion current flowing at a positive applied potential, the current is mainly carried by cations (Fig. 1(b)); a synthetic conical nanochannel with a positively charged surface rectifies the current such that the ion current flowing at a positive applied potential overwhelms the ion current flowing at a negative applied potential, the current is mainly carried by anions (Fig. 1(b)). A large current exhibited by asymmetrical nanochannel with positive surface charge (or negative surface charge) is referred to as “on” state and a small current is referred to as “off” state. Ion current rectification ( $R_p$ ) which describes the ion selectivity of a conical nanochannel can be defined as the absolute ratio of the current for an “on” state to the current for an “off” state measured at the same absolute value of the voltage but of opposite polarity.

In order to verify the successful fabrication of a nanochannel in a PET membrane, the PET foil after asymmetrical etching was sandwiched between two compartments containing buffer solution and transmembrane potentials from  $-6$  V to  $+6$  V were scanned with steps of  $0.15$  v/s. The current–voltage curve obtained from the nascent nanochannel with a tip diameter of  $1.5$  nm has the same characteristics as expected for an asymmetrical nanochannel grafted with a carboxylic group (Fig. 2(b), black curve). The current–voltage curve shows an “on” state at a negatively applied potential and shows an “off” state at a positively applied potential. After replacing the buffer solution (20 mM PBS with pH 9, 10 mM KCl) with the same buffer solution containing  $2\mu\text{M}$  Zn-DIGP (Fig. 2(a), red curve), the shape of the current–voltage curve was almost reversed, with the nonlinear profile featuring the asymmetrical conically shaped nanochannel with a positive surface charge, revealing that the negative surface charge on the surface of the nanochannel was overcompensated by adsorbing a positively charged Zn-DIGP onto the inner surface of the nanochannel. It has been proven that adsorption of a hydrophobic drug with positive charge polarity onto the tip side of the nanochannel induced local charge inversion in the nanopore wall, leading to switching of the ion selectivity of the nanochannel from a positive ion to a negative ion.<sup>7</sup> Therefore, the nanochannel we fabricated herein possessed the unique characteristics of an asymmetrical conically shaped nanochannel: a positively charged nanochannel was selective to anions, a negatively charged nanochannel was selective to cations.

The conically shaped nanochannel with a carboxylic group has long been reported to be responsive to the pH values. At pH close to the  $pK_a$  value ( $3.8$ ) of a carboxylic group on the surface of PET,<sup>62</sup> it has been reported that the surface charge was diminished, leading to a linear  $I$ – $V$  curve of the membrane containing a conically shaped nanochannel with the neutral surface. At pH above this isoelectric point, the surface charge is negative due to deprotonation of the carboxylic group, leading to a nonlinear

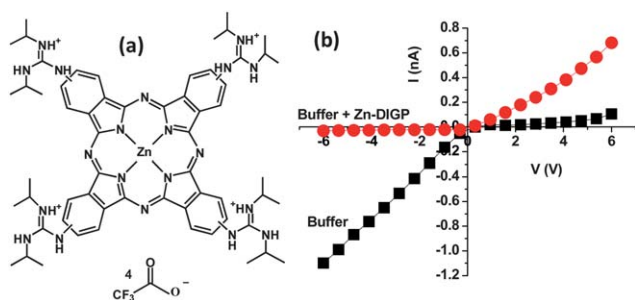


**Fig. 2** (a) Zn-DIGP; (b) current–voltage curves of the nanochannel in the presence of  $2\mu\text{M}$  Zn-DIGP (red circle) and in the absence of Zn-DIGP (black square), the small molecules were dissolved in 20 mM PBS buffer solution (pH 9) containing 10 mM KCl. The diameters of the narrow opening and the big opening of the nanochannel are 1.5 nm and 550 nm, respectively.

$I$ - $V$  curve. It has to be noted that in most cases,<sup>1,6</sup> salt concentration above 0.1 M KCl has been used to measure the  $I$ - $V$  curves of the nanochannel in solutions at pH values close to the  $pK_a$  value of a carboxylic group and to construct various nanochannel devices. In this way, important information regarding the surface property of the nascent nanochannel may be omitted due to a small Debye length under high concentration of salt, especially for nanochannel with a weakly charged surface. Therefore, for our experiments with the nanochannel obtained through the two-step etching method, we adopted various buffer solutions containing 10 mM KCl (10 mM PBS or 10 mM Tris-HCl or 10 mM HEPES), which was adjusted to different pH values by concentrated HCl.

As shown in Fig. 3(a), the  $I$ - $V$  curves obtained from a nanochannel with a tip diameter of 3 nm show that at a voltage scan range from  $-1$  V to  $1$  V, the nanochannel being immersed in 20 mM PBS buffered solution at pH 9 (or pH 5) revealed the characteristics of a nanochannel with a negative surface charge, which was consistent with those found in previous reports for a negatively charged surface;<sup>3,6</sup> when the membrane was immersed in 20 mM PBS buffer with pH 3, the  $I$ - $V$  curve of the nanochannel became linear at the same voltage range, illustrating that the negative surface charge was diminished as compared to the case at pH 9 (or pH 5). Most interestingly and contrary to previous studies, when we gradually extended the scan range beyond  $\pm 1$  V (Fig. 3(b)–3(f)), nonlinear  $I$ - $V$  curves for nanochannel in PET membrane sandwiched between buffer solution

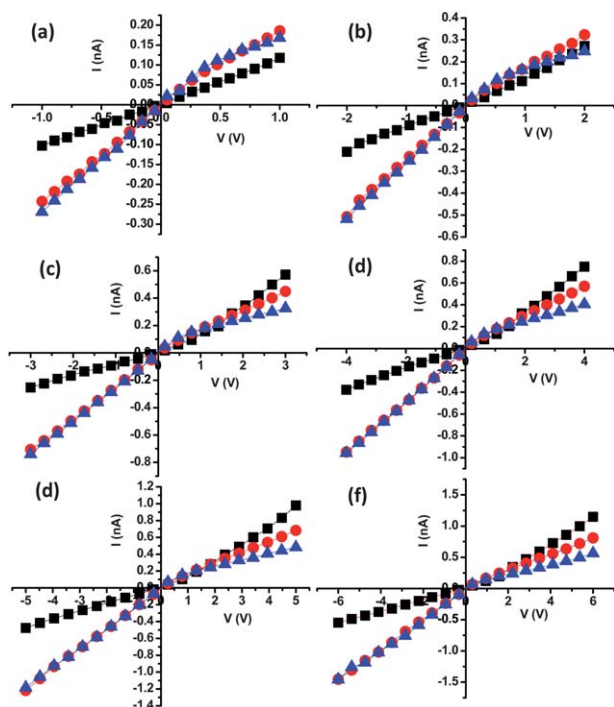


**Fig. 3** Current–voltage curves of the nanochannel with a scan range from  $-1$  V to  $1$  V (a),  $-2$  V to  $2$  V (b),  $-3$  V to  $3$  V (c),  $-4$  V to  $4$  V (d),  $-5$  V to  $5$  V (e) and  $-6$  V to  $6$  V (f), respectively. Buffer solutions at various pH values of 3 (black square), 5 (red circle) and 9 (blue triangle), containing 20 mM PBS and 10 mM KCl; the diameters of the narrow opening and the big opening of the nanochannel are 3 nm and 550 nm, respectively.

at pH 3, showed up with features as expected for a positive surface charge, revealing that the impact of a weakly charged surface in the nanochannel on ion current transport can only be observed at a higher transmembrane potential. Therefore, three requirements have to be met before observation of the impact of a weakly charged surface on the ion transport of the nanochannel: large voltage scan range, proper ionic strength and pH value of the electrolyte solution. To prove that the density of the positive surface charge was tunable, we measured the  $I$ - $V$  curves for the same nanochannel in 20 mM PBS buffered solution containing 10 mM KCl at pH values of 2.5, 1.9 and 1.4 (Fig. 4). In agreement with our deduction, the slopes of the  $I$ - $V$  curves at a positively applied potential increased with decreasing the pH values, demonstrating that the charge density of positive charge polarity on the nanochannel surface was highly adjustable. Although the rectification degree for the nanochannel in a solution of pH 1.4 decreased, which can be ascribed to the increased ionic conductivity of the solution ( $41.3 \text{ ms cm}^{-1}$ ) as compared to the lower ionic conductivity of a solution of pH 3 ( $9.24 \text{ ms cm}^{-1}$ ), the nonlinear behavior of  $I$ - $V$  curve as expected for nanochannel with a positive surface charge was still very clear. One important feature for the nanochannel with a charged surface is that the value of ionic current rectification increases along with increasing voltage. As shown in Fig. 5, the rectification ratio ( $R_f$ ), which is defined as the ratio of the current corresponding to the “on” state to the current corresponding to the “off” state, increased with increasing transmembrane potential in solutions at pH 2.5 and pH 9 (or pH 5). However, the rectification ratio just slightly increased if the membrane containing nanochannel was sandwiched between solutions at pH 3. It has to be noted that all the data for each pH value were obtained from one big voltage scan instead of a series of voltage scans. These results further confirmed that the surface of the nanochannel after wet-chemistry etching possessed the capability of switching the charge polarity among the three states by simply adjusting the pH value of surrounding environment. Since the

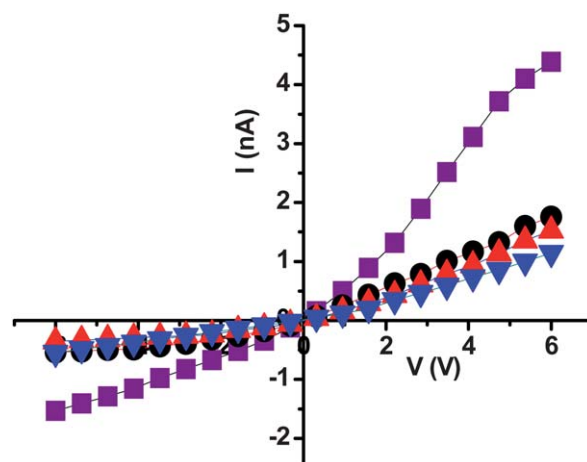


**Fig. 4** Current–voltage curves of the nanochannel with a voltage range from  $-6$  V to  $6$  V. Buffer solutions at various pH values of 1.4 (purple square), 1.9 (black circle), 2.5 (red upper triangle) and 3.0 (blue down triangle), containing 20 mM PBS and 10 mM KCl. The diameters of the narrow opening and the big opening of the nanochannel are 3 nm and 550 nm, respectively.

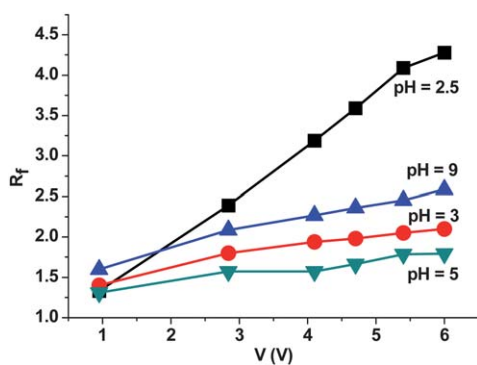


**Fig. 5** Plots of voltage-dependent ion current rectification at 20mM PBS buffered solution containing 10 mM KCl at pH 2.5 (black square), pH 3 (red circle), pH 5 (grey down triangle), pH 9 (blue upper triangle). The diameters of the narrow opening and the big opening of the nanochannel are 1.5 nm and 550 nm, respectively.

surface of PET membrane after wet-chemistry etching is grafted with carboxylic group, hydrogen bonded hydrogel layer *via* dimerization of carboxylic acid may exist in the nanopore surface.<sup>63</sup> Therefore, we assume that at low pH values below 3, further protonation of the hydrogel layer can contribute to the accumulation of a positive charge in the nanochannel wall.

To confirm where if buffer solution can influence our experimental results, three kinds of buffer solution at various pH values were used to characterize another nascent nanochannel membrane with tip diameter of 1.5 nm and base diameter of 550 nm. Indeed, as shown in Fig. 6, all buffer solutions at pH 2 used to measure the  $I$ - $V$  curves of the same nanochannel produced the same trend as those in Fig. 3 and 4. By comparing the  $I$ - $V$  curves obtained with buffers Tris and Hepes at pH 6, Hepes can be adsorbed onto the surface of the nanochannel, leading to a positive surface charge at pH 6 (Fig. 6(c)). Therefore, for Hepes buffer at pH value of 2, the positive surface charge was ascribed to the adsorption of Hepes and protonation of the carboxyl group. In combination with their corresponding plots of voltage-dependent ion current rectification (Fig. 6(b), 6(d) and 6(f)), a low pH value can totally switch the charge polarity of the nanochannel from negative to positive without tedious modification. In order to further validate our point that the inner wall of the nanochannel can be positively charged at a low pH value, aqueous HCl solution of pH 2 was used to characterize the same membrane (Fig. 7), which excluded any possibility of adsorption of contaminant. The  $I$ - $V$  curve obtained from the nanochannel with a tip diameter of 1.5 nm clearly shows the characteristics as expected for a conically shaped nanochannel with a positive surface charge.

Finally, we fabricated another asymmetrical conical nanochannel with 30 nm diameter of the narrow opening using the surfactant-protected one-step etching method, which has been claimed to produce better quality of conically shaped nanochannels.<sup>1</sup> Indeed, we observed significant ion current rectification of the nascent nanochannel. It has to be noted that surfactant 2A1 has been used in the whole etching process. As shown in Fig. 8(a) (black curve), without washing the nascent nanochannel with ethanol solution, addition of aqueous HCl solution at pH 2 did not produce rectification properties as

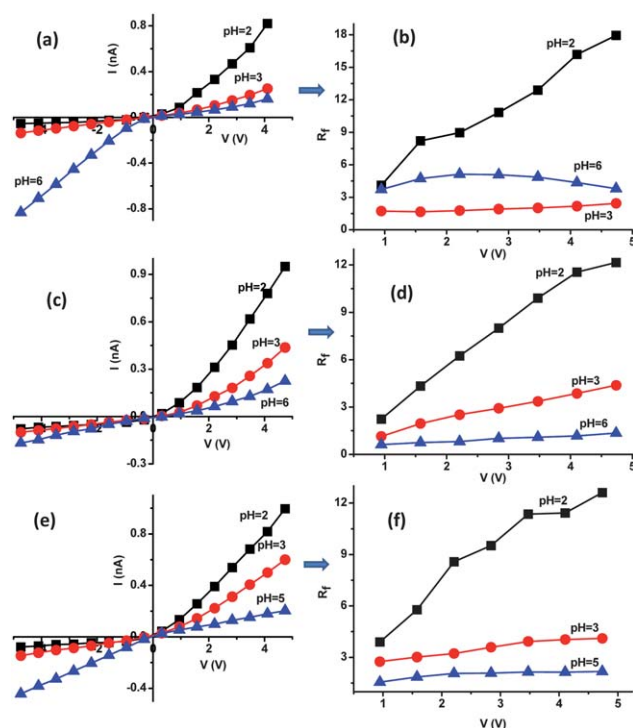


**Fig. 6** Current–voltage curves of the nanochannel with a scan range from  $-4.73$  V to  $4.73$  V in different buffer solutions: 10 mM Tris with 10 mM KCl (a), 10 mM Hepes with 10 mM KCl (c), 20 mM PBS with 10 mM KCl (e). Plots of a voltage-dependent ion current rectification ratio (b, d and f) correspond to the current–voltage curves (a, c and e). The diameters of the narrow opening and the big opening of the nanochannel are 1.5 nm and 550 nm, respectively.

expected for a nanochannel with a positive surface charge. In contrast, it produced ion current rectification as expected for a nanochannel with a negative surface charge. Considering that it was highly possible that surfactant 2A1 having two negative charges can be adsorbed onto the polymer surface, we reasoned that this kind of ion current rectification was due to negative charges of surfactant 2A1 which has not been fully removed even after washing with plenty of water. Therefore, we immersed the membrane in a pure ethanol solution overnight. Measurement of the  $I$ - $V$  curve showed that in an aqueous HCl solution of pH 2, the nanochannel after removal of surfactant 2A1 significantly

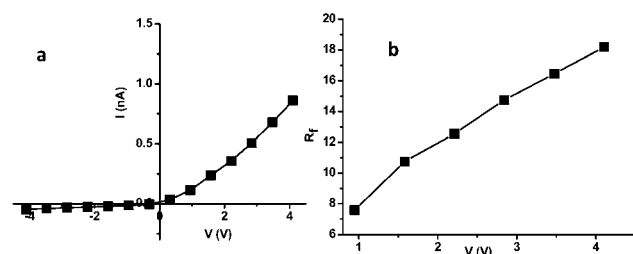


**Fig. 7** Current–voltage curves of the nanochannel with a scan range from  $-4.1$  V to  $4.1$  V in aqueous HCl solution at pH 2 (a) and the correspondingly voltage-dependent ion current rectification ratio (b). The diameters of the narrow opening and the big opening of the nanochannel are 1.5 nm and 550 nm, respectively.

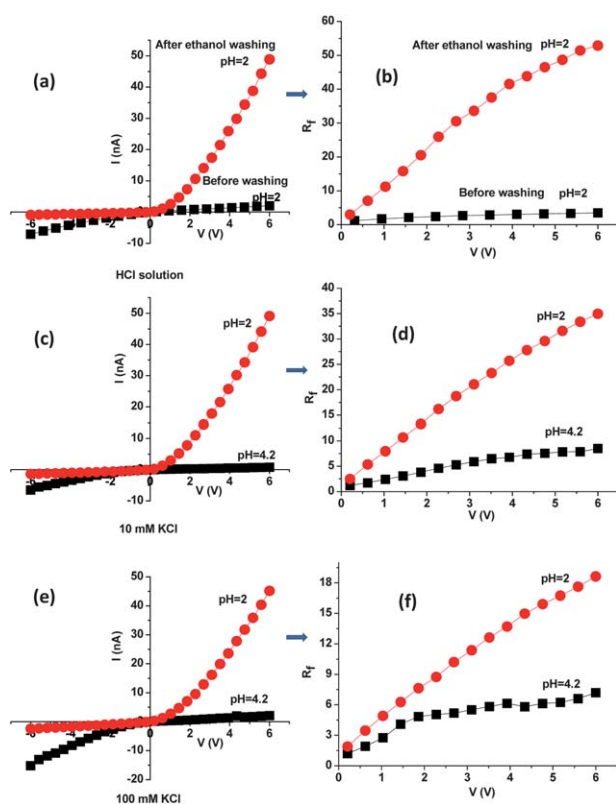


**Fig. 8** Current–voltage curves of the nanochannel fabricated using the surfactant-protected one-step etching method and the corresponding plot of voltage-dependent ion current rectification. (a) Current–voltage curve measured in aqueous HCl solution of pH 2 before ethanol washing (black) and after ethanol washing (red). (c) Current–voltage curve measured in 10 mM KCl solutions at pH 2 (red) and at pH 4.2 (black). (e) Current–voltage curves measured in 100 mM KCl solutions at pH 2 (red) and at pH 4.2 (black). (b, d and f) Corresponding plots of the voltage-dependent ion current rectification ratio (red for pH 2, black for pH 4.2). All solutions were adjusted to the desired pH values by concentrated HCl. The diameters of the narrow opening and the big opening of the conical nanochannel are 30 nm and 200 nm, respectively.

rectified the current in the direction as expected for a nanochannel with a positive charge (Fig. 8(a), red curve). The ion rectification ratio can reach 53 at an absolute voltage value of 6 V as shown in Fig. 8(b) (red curve). So, the reversal of the surface charge in the nanochannel wall indeed happened after the surface-adsorbed surfactant with a negative charge had been eliminated.

Other functional properties possessed by the as-prepared conical nanochannel without surface-adsorbed surfactant have also been tested. As shown in Fig. 8(c)–8(f), an asymmetrical conical nanochannel rectified the current in opposite directions in KCl solution at pH 2 and pH 4.2, which was consistent with the results described above by using a nanochannel obtained using the two-step etching method. The high ionic strength decreased the ion current rectification, which is also clearly shown in Fig. 8(d) and 8(f). In one word, the nanochannel fabricated herein has the same physical and chemical properties as others, responsive to the pH values of the surrounding environments and ionic strength of electrolyte solution.

Therefore, in this study, we discovered that the  $I$ – $V$  curve of the nanochannel in a solution of  $\text{pH} \leq 3$  clearly showed the nonlinear ion current from which the ion current rectification (as expected for a nanochannel with a positive surface charge) can be obtained. This interesting phenomenon, to the best of our knowledge, was paid enough attention for the first time, indicating that fabricating nanofluidic diode dispenses with the modification steps which were previously used to confer a positive charge to the surface wall of nanochannels in the PET membrane.

## 4. Conclusions

In summary, this study has demonstrated that an asymmetrical conically shaped nanochannel in the PET membrane had the capability of switching the surface charge polarity from negative to positive, leading to formation of a nanofluidic diode without any modification and without the existence of a heavy metal ion. In order to observe this interesting phenomenon, proper ion strength and low pH values have to be used. We believe our study enriches the knowledge of nanochannel technology which has attracted significant attention in the past years. Our result complements the previous studies which traditionally considered that a conically shaped nanochannel in a PET membrane sandwiched between two buffer solutions at  $\text{pH} \leq 3$  exhibited no rectification, and if any, much weaker rectification than that for negatively charged surface, since the surface charge on the membrane was considered to approach zero with decreasing the pH value of the buffer solution down to the  $\text{pK}_a$  of carboxylic acid. Nevertheless, in this study, we discovered that in the buffer solution at low pH values and with a proper ionic strength, the conically shaped nanochannel with a small diameter of the narrow opening exhibited distinct ion current rectification, as expected for a nanochannel with a positive surface charge. We reasoned that the current rectification engendered by the positive charge of the surface of a conical nanochannel was due to further protonation of the neutralized carboxylic acid or the hydrogen bonded gel-layer inside the nanochannel. Therefore, pH-reversed ionic-current rectification *via* a conical nanochannel can be achieved without any modification of the PET membrane, facilitating the easy fabrication of a nanofluidic diode in future applications.

## Acknowledgements

This work was supported by the National Natural Science Foundation of China (No. 20905056 and 21075120), 973 Project (2009CB930100 and 2010CB933600). We also like to acknowledge Prof. Nathan W. Luedtke, University of Zurich, for his assistance in providing the Zn-DIGP sample.

## References

- 1 M. Ali, V. Bayer, B. Schiedt, R. Neumann and W. Ensinger, *Nanotechnology*, 2008, **19**, 485711–485719.
- 2 C. C. Harrell, Z. S. Siwy and C. R. Martin, *Small*, 2006, **2**, 194–198.
- 3 Y. He, D. Gillespie, D. Boda, I. Vlassiok, R. S. Eisenberg and Z. S. Siwy, *J. Am. Chem. Soc.*, 2009, **131**, 5194–5202.
- 4 X. Hou, F. Yang, L. Li, Y. L. Song, L. Jiang and D. B. Zhu, *J. Am. Chem. Soc.*, 2010, **132**, 11736–11742.

- 5 P. Jin, H. Mukaibo, L. P. Horne, G. W. Bishop and C. R. Martin, *J. Am. Chem. Soc.*, 2010, **132**, 2118–2119.
- 6 Z. S. Siwy, *Adv. Funct. Mater.*, 2006, **16**, 735–746.
- 7 J. Wang and C. R. Martin, *Nanomedicine*, 2008, **3**, 13–20.
- 8 Y. B. Xie, J. M. Xue, L. Wang, X. W. Wang, K. Jin, L. Chen and Y. G. Wang, *Langmuir*, 2009, **25**, 8870–8874.
- 9 B. Yameen, M. Ali, R. Neumann, W. Ensinger, W. Knoll and O. Azzaroni, *J. Am. Chem. Soc.*, 2009, **131**, 2070–2071.
- 10 M. X. Macrae, S. Blake, M. Mayer and J. Yang, *J. Am. Chem. Soc.*, 2010, **132**, 1766–1767.
- 11 Z. Siwy, D. Dobrev, R. Neumann, C. Trautmann and K. Voss, *Appl. Phys. A: Mater. Sci. Process.*, 2003, **76**, 781–785.
- 12 T. Z. Butler, M. Pavlenok, I. M. Derrington, M. Niederweis and J. H. Gundlach, *Proc. Natl. Acad. Sci. U. S. A.*, 2008, **105**, 20647–20652.
- 13 M. Chen, S. Khalid, M. S. P. Sansom and H. Bayley, *Proc. Natl. Acad. Sci. U. S. A.*, 2008, **105**, 6272–6277.
- 14 I. M. Derrington, T. Z. Butler, M. D. Collins, E. Manrao, M. Pavlenok, M. Niederweis and J. H. Gundlach, *Proc. Natl. Acad. Sci. U. S. A.*, 2010, **107**, 16060–16065.
- 15 E. Garcia-Gimenez, A. Alcaraz, V. M. Aguilera and P. Ramirez, *J. Membr. Sci.*, 2009, **331**, 137–142.
- 16 S. Howorka, L. Movileanu, O. Braha and H. Bayley, *Proc. Natl. Acad. Sci. U. S. A.*, 2001, **98**, 12996–13001.
- 17 Y. Jung, H. Bayley and L. Movileanu, *J. Am. Chem. Soc.*, 2006, **128**, 15332–15340.
- 18 X. F. Kang, S. Cheley, X. Y. Guan and H. Bayley, *J. Am. Chem. Soc.*, 2006, **128**, 10684–10685.
- 19 H. C. Wu, Y. Astier, G. Maglia, E. Mikhailova and H. Bayley, *J. Am. Chem. Soc.*, 2007, **129**, 16142–16148.
- 20 I. Vlasiouk, T. R. Kozel and Z. S. Siwy, *J. Am. Chem. Soc.*, 2009, **131**, 8211–8220.
- 21 M. Tagliazucchi, O. Azzaroni and I. Szleifer, *J. Am. Chem. Soc.*, 2010, **132**, 12404–12411.
- 22 M. Ali, B. Yameen, R. Neumann, W. Ensinger, W. Knoll and O. Azzaroni, *J. Am. Chem. Soc.*, 2008, **130**, 16351–16357.
- 23 L. T. Sexton, L. P. Horne, S. A. Sherrill, G. W. Bishop, L. A. Baker and C. R. Martin, *J. Am. Chem. Soc.*, 2007, **129**, 13144–13152.
- 24 Z. Siwy, L. Trofin, P. Kohli, L. A. Baker, C. Trautmann and C. R. Martin, *J. Am. Chem. Soc.*, 2005, **127**, 5000–5001.
- 25 Z. S. Siwy, M. R. Powell, A. Petrov, E. Kalman, C. Trautmann and R. S. Eisenberg, *Nano Lett.*, 2006, **6**, 1729–1734.
- 26 C. Wei, A. J. Bard and S. W. Feldberg, *Anal. Chem.*, 1997, **69**, 4627–4633.
- 27 L. X. Zhang, X. H. Cao, Y. B. Zheng and Y. Q. Li, *Electrochem. Commun.*, 2010, **12**, 1249–1252.
- 28 E. N. Ervin, R. Kawano, R. J. White and H. S. White, *Anal. Chem.*, 2008, **80**, 2069–2076.
- 29 E. N. Ervin, R. J. White and H. S. White, *Anal. Chem.*, 2009, **81**, 533–537.
- 30 J. Y. Feng, J. Liu, B. H. Wu and G. L. Wang, *Anal. Chem.*, 2010, **82**, 4520–4528.
- 31 C. L. Gao, S. Ding, Q. L. Tan and L. Q. Gu, *Anal. Chem.*, 2009, **81**, 80–86.
- 32 D. A. Jayawardhana, J. A. Crank, Q. Zhao, D. W. Armstrong and X. Y. Guan, *Anal. Chem.*, 2009, **81**, 460–464.
- 33 M. Karhanek, J. T. Kemp, N. Pourmand, R. W. Davis and C. D. Webb, *Nano Lett.*, 2005, **5**, 403–407.
- 34 J. H. Shim, J. Kim, G. S. Cha, H. Nam, R. J. White, H. S. White and R. B. Brown, *Anal. Chem.*, 2007, **79**, 3568–3574.
- 35 L. J. Steinbock, O. Otto, C. Chimere, J. Gornall and U. F. Keyser, *Nano Lett.*, 2010, **10**, 2493–2497.
- 36 S. Umehara, M. Karhanek, R. W. Davis and N. Pourmand, *Proc. Natl. Acad. Sci. U. S. A.*, 2009, **106**, 4611–4616.
- 37 S. Umehara, N. Pourmand, C. D. Webb, R. W. Davis, K. Yasuda and M. Karhanek, *Nano Lett.*, 2006, **6**, 2486–2492.
- 38 G. L. Wang, B. Zhang, J. R. Waymott, J. M. Harris and H. S. White, *J. Am. Chem. Soc.*, 2006, **128**, 7679–7686.
- 39 R. J. White, E. N. Ervin, T. Yang, X. Chen, S. Daniel, P. S. Cremer and H. S. White, *J. Am. Chem. Soc.*, 2007, **129**, 11766–11775.
- 40 R. J. White, B. Zhang, S. Daniel, J. M. Tang, E. N. Ervin, P. S. Cremer and H. S. White, *Langmuir*, 2006, **22**, 10777–10783.
- 41 B. Zhang, Y. H. Zhang and H. S. White, *Anal. Chem.*, 2006, **78**, 477–483.
- 42 M. Ali, B. Yameen, J. Cervera, P. Ramirez, R. Neumann, W. Ensinger, W. Knoll and O. Azzaroni, *J. Am. Chem. Soc.*, 2010, **132**, 8338–8348.
- 43 M. Ali, B. Schiedt, K. Healy, R. Neumann and A. Ensinger, *Nanotechnology*, 2008, **19**, 85713–85718.
- 44 Y. Choi, L. A. Baker, H. Hillebrener and C. R. Martin, *Phys. Chem. Chem. Phys.*, 2006, **8**, 4976–4988.
- 45 F. Xia, W. Guo, Y. D. Mao, X. Hou, J. M. Xue, H. W. Xia, L. Wang, Y. L. Song, H. Ji, O. Y. Qi, Y. G. Wang and L. Jiang, *J. Am. Chem. Soc.*, 2008, **130**, 8345–8350.
- 46 X. Hou and L. Jiang, *ACS Nano*, 2009, **3**, 3339–3342.
- 47 X. Hou, H. Dong, D. B. Zhu and L. Jiang, *Small*, 2010, **6**, 361–365.
- 48 X. Hou, W. Guo and L. Jiang, *Chem. Soc. Rev.*, 2011, **40**, 2385–2401.
- 49 X. Hou, Y. J. Liu, H. Dong, F. Yang, L. Li and L. Jiang, *Adv. Mater.*, 2010, **22**, 2440–2443.
- 50 X. Hou, W. Guo, F. Xia, F. Q. Nie, H. Dong, Y. Tian, L. P. Wen, L. Wang, L. X. Cao, Y. Yang, J. M. Xue, Y. L. Song, Y. G. Wang, D. S. Liu and L. Jiang, *J. Am. Chem. Soc.*, 2009, **131**, 7800–7805.
- 51 L. T. Sexton, H. Mukaibo, P. Katira, H. Hess, S. A. Sherrill, L. P. Horne and C. R. Martin, *J. Am. Chem. Soc.*, 2010, **132**, 6755–6763.
- 52 K. M. Zhou, M. L. Kovarik and S. C. Jacobson, *J. Am. Chem. Soc.*, 2008, **130**, 8614–8616.
- 53 H. Mukaibo, L. P. Horne, D. Park and C. R. Martin, *Small*, 2009, **5**, 2474–2479.
- 54 S. B. Lee and C. R. Martin, *Anal. Chem.*, 2001, **73**, 768–775.
- 55 R. I. Zalewski, *Bull. Acad. Polon. Sci., Ser. Sci. Chem.*, 1972, **20**, 853.
- 56 C. F. Wells, *J. Phys. Chem.*, 1973, **77**, 1994–1996.
- 57 Z. Geltz, H. Kokocinska, R. I. Zalewski and T. M. Krygowski, *J. Chem. Soc., Perkin Trans. 2*, 1983, 1069–1070.
- 58 R. Stewart and K. Yates, *J. Am. Chem. Soc.*, 1960, **82**, 4059–4061.
- 59 J. Alzeer, B. R. Vummidi, P. J. C. Roth and N. W. Luedtke, *Angew. Chem., Int. Ed.*, 2009, **48**, 9362–9365.
- 60 J. E. Wharton, P. Jin, L. T. Sexton, L. P. Horne, S. A. Sherrill, W. K. Mino and C. R. Martin, *Small*, 2007, **3**, 1424–1430.
- 61 Z. S. Siwy and S. Howorka, *Chem. Soc. Rev.*, 2010, **39**, 1115–1132.
- 62 L. E. Ermakova, M. P. Sidorova and M. E. Bezrukova, *Colloid J.*, 1998, **60**, 705–712.
- 63 J. Xue, Y. Xie, Y. Yan, J. Ke and Y. Wang, *Biomicrofluidics*, 2009, **3**, 22408.